

# Characterization of Selective Polysilicon Deposition for MEMS Resonator Tuning

Daphne Joachim, *Member, ASME*, and Liwei Lin, *Member, IEEE*

**Abstract**—Variations in micromachining processes cause submicron differences in the size of MEMS devices, which leads to frequency scatter in resonators. A new method of compensating for fabrication process variations is to add material to MEMS structures by the selective deposition of polysilicon. It is performed by electrically heating the MEMS in a 25 °C silane environment to activate the local decomposition of the gas. On a  $(1.0 \times 1.5 \times 100) \mu\text{m}^3$ , clamped-clamped, polysilicon beam, at a power dissipation of 2.38 mW (peak temperature of 699 °C), a new layer of polysilicon (up to 1  $\mu\text{m}$  thick) was deposited in 10 min. The deposition rate was three times faster than conventional LPCVD rates for polysilicon. When selective polysilicon deposition (SPD) was applied to the frequency tuning of specially-designed, comb-drive resonators, a correlation was found between the change in resonant frequency and the length of the newly deposited material (the hotspot) on the resonator's suspension beams. A second correlation linked the length of the hotspot to the magnitude of the power fluctuation during the deposition trial. In one sample, at a power dissipation of 10.7 mW (peak temperature of 800 °C), the cross section of a suspension beam increased from 6 to 9.4  $\mu\text{m}^2$  in 15 min. The resonant frequency increased 1.96% from its initial value of 86.6 kHz. This change was in good agreement with the value of 2.2% predicted in a simulation. The mechanisms for changing resonant frequency by the SPD process include increasing mass and stiffness and altering residual stress. The effects of localized heating are presented. The experiments and simulations in this work yield guidelines for tuning resonators to a target frequency. [802]

**Index Terms**—High-temperature thermal conductivity of polysilicon, Multi User MEMS Processes (MUMPs), postfabrication processing, residual stress, resonant frequency tuning, trimming.

## I. INTRODUCTION

PROCESS variations occur in the fabrication of MEMS, making postfabrication modifications necessary to increase yield and produce devices to design specifications. When the structural materials of MEMS are not deposited uniformly or etched accurately, the resulting devices have differences in properties such as electrical resistance, mechanical deflection under load or natural frequency. One of the techniques of compensating for fabrication process variations is laser trimming [1], in which parts of a structure are removed.

Manuscript received January 15, 2002; revised August 28, 2002. This work was supported under the University of Michigan Rackham Merit Fellowship and Research Grant # F30602-98-2-0227 from DARPA. This paper appeared in part in the conference proceedings of the 2001 ASME IMECE MEMS Symposium and the 2002 IEEE MEMS Conference. Subject Editor G. K. Fedder.

D. Joachim was with the Mechanical Engineering Department, University of Michigan, Ann Arbor, MI 48109 USA. She is now with Sandia National Laboratories, Livermore, CA 94551 USA (e-mail: djoachi@sandia.gov).

L. Lin is with the Mechanical Engineering Department, University of California, Berkeley, CA 94720 USA.

Digital Object Identifier 10.1109/JMEMS.2003.809967

However, laser trimming is not feasible for very small structures ( $< 10 \mu\text{m}$  wide), because costly, specialized lasers are required for such precise work. A new method, demonstrated here, for compensating for fabrication process variations is to add material to MEMS structures by the selective deposition of polysilicon. Selective polysilicon deposition is performed by locally heating the MEMS structures in a silane environment, as shown in Fig. 1. Selective polysilicon deposition may also be used in welding assembled MEMS components, or tuning the frequency of microresonators, which will be discussed later.

Selective deposition has previously been used in the fabrication of MEMS gas sensors [2]–[4]. Platinum was selectively deposited on components of the gas sensors because chemically etching the metal would have destroyed its properties. The process was performed by electrically heating surface and bulk micromachined, polysilicon, rectangular beams and circular membranes in various platinum precursor gasses. In the present work, the precursor gas is silane, which is widely available in microfabrication facilities. Another major difference in the processes is the temperature range in which the precursor decomposition reactions were performed: 200 °C–450 °C, in [2]–[4] for platinum deposition, and 600–800 °C, here, to produce polysilicon. Therefore, the heat transfer and mechanical analyzes of the substrates in this work are dependent on the high-temperature properties of polysilicon. These are still not well known for thin-film polysilicon, but values that produce consistent results are deduced from comparison of experimental and simulated data, as shown below.

The methods of selectively depositing polysilicon include laser writing [5] and epitaxial growth in specially prepared windows on a wafer [6]. The selective deposition of polysilicon by silane decomposition on electrically heated, released microstructures, presented here, is a new process.

Selective polysilicon deposition (SPD) will be applied to frequency tuning of comb-drive resonators. Fabricating high frequency microresonators at precise frequencies is difficult because they are relatively small and significantly affected by submicron variations in size. Existing MEMS frequency tuning methods include electronic tuning by varying the dc-bias voltage [7]; localized annealing [8]; and etching/ion milling [9]. Electronic tuning can be used in service, but introduces parasitic capacitance to the system. Localized annealing is similar to the present method, in that a resonator is electrically heated, but changing resonant frequency by heating alone relies on modifying the residual stress of the rotor, which is difficult to control. The change in resonant frequency is not predictable. In the etching/ion milling process, material is removed from all surfaces, on and around the resonator.

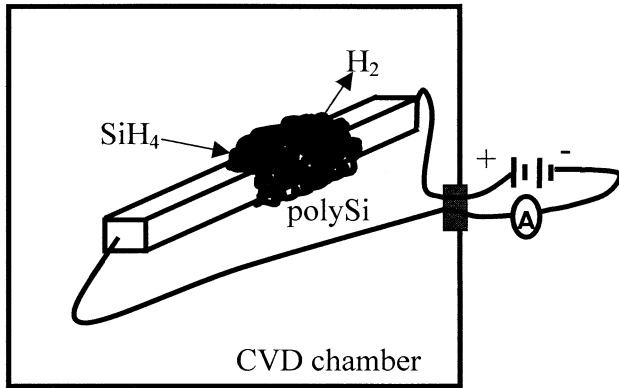


Fig. 1. Schematic of the selective polysilicon deposition (SPD) process.

Reducing the comb-finger, reduces the capacitance of the resonator. Frequency tuning using SPD does not have these drawbacks, but requires adequate facilities to handle the silane.

The SPD process was developed using suspended microbeams with fixed-fixed supports [10], then it was applied to comb-drive resonators for frequency tuning [11], [12]. In this paper, the SPD process is demonstrated on a microbeam resonator (a microbeam with electrodes along side, as shown in Fig. 2); there is a comparison of frequency tuning of comb-drive resonators using the SPD and localized annealing processes; and the mechanisms for modifying resonant frequency by adding material in a thermal process are analyzed.

## II. DEVELOPMENT OF SPD

The selective deposition of polysilicon occurs by the thermal decomposition of silane gas on locally heated microstructures. The silane decomposition reaction,  $\text{SiH}_{4(g)} \Rightarrow \text{Si}_{(s)} + 2\text{H}_{2(g)}$ , requires a temperature of at least  $420^\circ\text{C}$  to proceed [13]. The temperature required to obtain deposition was much higher. To reduce complexity, the intermediate reactions in the decomposition chemistry were neglected. This assumption was validated by the deposition results obtained under various process conditions [14]. The key to regulating the selective deposition process is controlling the temperature of the substrate, the microbeam. This, essentially, requires predicting the electrical current to create sufficient Joule heating to reach the temperatures for deposition. The use of very small microbeams ( $1\ \mu\text{m}$  wide) at high temperatures and the uncertainty about the properties of polysilicon make precise predictions of the electrical input difficult. A simple method of estimating the required current, neglecting nonlinear changes in resistance and radiation, was to use the formula:  $I[\text{mA}] = \sqrt{P/((1 + \alpha \cdot \Delta T)R_o)}$ , where  $P[\text{mW}]$  is the power dissipation to obtain deposition (found experimentally; dependent on the size of the substrate);  $\alpha$  is the temperature coefficient of resistance of the polysilicon microbeam (found to be  $1.5 \times 10^{-3}/^\circ\text{C}$  when measured from  $25$  to  $400^\circ\text{C}$ );  $\Delta T$  (taken to be  $600^\circ\text{C}$ ) is the desired deposition temperature minus the initial temperature; and  $R_o$  is the initial resistance of the sample. Note that the predicted current changes for samples of nominally the same size when their initial resistances differ. Once the current level required to reach deposition temperatures was predicted, a deposition trial was attempted. The following is the experimental procedure for and typical results of the SPD process.

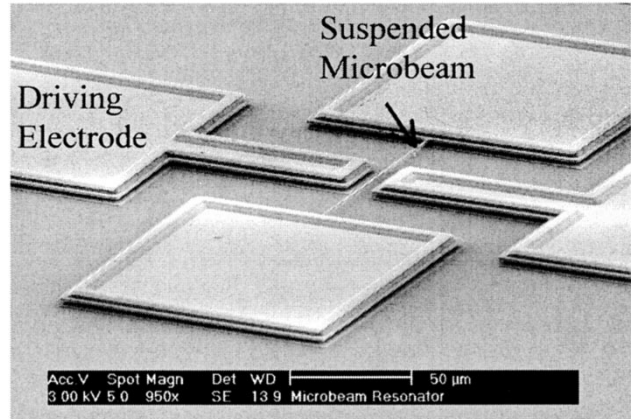


Fig. 2. The microbeam resonator.

### A. Procedure

Microbeam resonators were fabricated using the Cronos Multi User MEMS Processes (MUMPs) [15], in the phosphorus-doped polysilicon (Poly2) layer by surface-micromachining. The structure shown in Fig. 2 was Sample A. The beam was  $1.5\ \mu\text{m}$  thick,  $1.0\ \mu\text{m}$  wide, and  $100\ \mu\text{m}$  long. It was suspended  $2.75\ \mu\text{m}$  above a silicon-nitride coated, silicon wafer. Its initial resistance was  $2280\ \Omega$ . The microbeam can be driven electrostatically using the adjacent electrodes. These electrodes were not used in the selective deposition trial. The sample was mounted on a dual-in-line package and connected to a power feedthrough in a plasma-enhanced chemical vapor deposition chamber. Standard features of the PECVD, such as the RF power and platen heater were not used because these sources of energy render global deposition. Silane was drawn into the chamber at  $80\ \text{sccm}$  to a total pressure of  $500\ \text{mtorr}$ . The silane supply was a mixture containing mostly the carrier gas, helium (90% by volume), which prescribes certain deposition rates. Sample A was connected to an HP semiconductor analyzer located outside the CVD chamber and a constant current of  $0.8\ \text{mA}$  was applied for  $10\ \text{min}$ . Heat was generated in the microbeam to activate the local decomposition of the silane. The output voltage was recorded and power dissipation was computed.

### B. Results and Discussion

Fig. 3(a) and (b) shows the selective deposition of polysilicon on the microbeam resonator. Deposition occurred on the portions of the microbeam that were above the silane decomposition temperature during the trial. The thickness of the new polysilicon corresponds to the temperature distribution along the microbeam. This indicates that the silane-decomposition reaction took place by the surface-reaction-limited mechanism, which gives a bound of  $\approx 900^\circ\text{C}$  on the peak temperatures. The location of the peak temperature is at the center of the microbeam—the new, thickest point. The sample had intentionally been tilted in the deposition chamber because this was observed to produce thicker deposits. The surface of the die was inclined toward the vertical. The flow of heat by natural convection [following the arrow on Fig. 3(b)] resulted in deposition asymmetric with respect to the axis of the microbeam. Another result was a small accumulation of polysilicon on an adjacent electrode. Gas

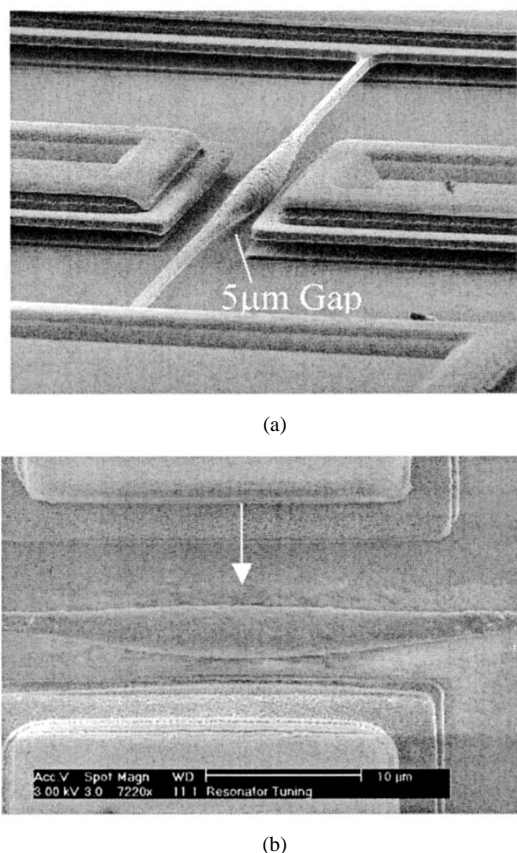


Fig. 3. Selectively deposited polysilicon on Sample A, where (a) is magnified 4400X and (b) is the top view.

phase decomposition of silane was ruled out because of the well defined gradient in deposition on the nearby electrode. Deposition would otherwise be scattered. The texture of the new polysilicon in Fig. 3 (a) and (b) was typical of other deposition trials [14], but variations in grain structure (long whiskers [10], [14]; spherical pebbles [12] and gnarled clumps [see Fig.8 (c)] occurred with changes in process temperature and surface chemistry. Despite variations in process conditions, and other structures on the die creating turbulence in the flow of the precursor, selective deposition of polysilicon was readily obtained on the heated microbeam.

During the deposition trial for Sample A, the peak power dissipation was 2.38 mW. An electrothermal finite element simulation was developed to determine the temperature of the microbeam from this datum [14]. The following properties were required:  $R_{\theta}$ ,  $\alpha$  and thermal conductivity,  $k$ . The boundary conditions were the input current from the experiment and a constant temperature of 25 °C at the anchors (because the relatively large substrate was taken as a heat sink). The thermal conductivity of polysilicon was determined from current-voltage tests on samples of similar size to Sample A. A room temperature value of 30 W/mK was found [14]. This is consistent with values found previously [16]. The output of the finite element simulation was voltage and temperature. The accuracy of the predicted temperature was measured by comparing the predicted output power to the experimental power dissipation. The  $\alpha$  and  $k$  were assumed to be 1.4 e-3/°C, 32 W/mK, respectively, to fit the simulation to the experimental data. In doing so, the calculated peak temperature for Sample A was

699 °C, which is consistent with the other evidence that SPD occurred by the surface-reaction-limited, silane-decomposition mechanism. Variations in the high-temperature, thermal conductivity of thin-film polysilicon have also been explored using SPD results and electro-thermal simulations [14]. Nearly constant thermal conductivity had to be used throughout the temperature range of the process to reproduce the power-dissipation profiles from the experiments.

Measuring the thickness of the selectively deposited polysilicon in Fig.3(a) and (b) gives a deposition rate at the center of the microbeam of approximately 100 nm/min. The epitaxial growth rate of silicon was reported to be 30 nm/min at 700 °C [17]. The discrepancy does not necessarily mean that the peak temperature for Sample A was higher. In the selective deposition of polysilicon with lasers, it was also reported that the temperature suggested by the deposition rate exceeded the temperature calculated by other means [18]. The SPD method may be much faster than the conventional, global, deposition process because of the presence of current in the substrate. It has been reported that charge at nucleation sites plays a role in the silane decomposition reaction [19].

To measure the natural frequency of the microbeam resonator, ac-voltage was applied to one of the adjacent electrodes and dc-voltage to the microbeam. Motion was induced at 779 kHz using 20 Vpp-ac and 120 V-dc, at atmospheric pressure. After selective deposition, detectable motion could not be induced in the microbeam at safe voltage levels. It had become stiffer. The effect of SPD on resonant frequency was measured in a second design, the special comb-drive resonator, which has higher capacitance.

### III. MODIFYING FREQUENCY BY SPD

To enable frequency tuning by selective polysilicon deposition, a resonator that could withstand the thermal stresses of the post-fabrication process (up to 800 °C) was designed. The tunable resonator had to be stiff enough to prevent buckling during heating but not so stiff that the original and modified resonant frequencies were above 100 kHz, which is the limit of the measurement technique described below. The layout of this special comb-drive resonator is shown in Fig. 4. Features of the device include a split ground plane to electrically isolate the anchors of the rotor, to allow current to be passed through it; and a single beam suspension on one side of the rotor. The current density and therefore temperature are greatest along the single beam, which makes the location of the new deposition predictable. A series of thermo-elastic and modal, finite element simulations were developed to find the dimensions satisfying the design criteria. In the final structure, all the beams were 3 μm wide, the four-beam suspension was 75 μm long and the single beam was 100 μm long.<sup>1</sup>

#### A. Procedure

The experimental procedure here differs in many respects from that described above. The special comb-drive resonators

<sup>1</sup>At these lengths, a simulation of the vibration mode shape shows a component of the rotor's displacement toward the four-beam suspension, but the device remains a lateral resonator [14]. If this design is used in a gyroscope, it will also be important to make the stiffness of the springs equal on both sides of the rotor.

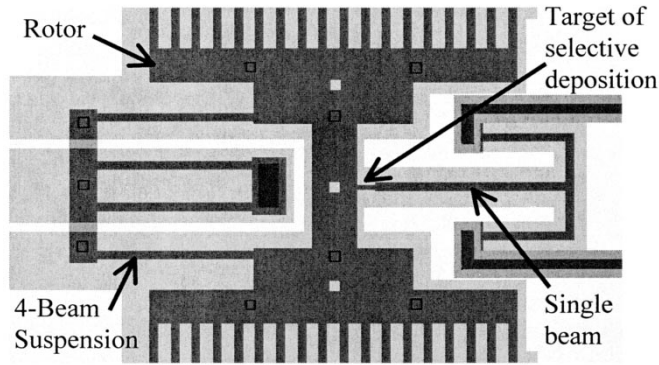


Fig. 4. Rotor of the special comb-drive resonator.

TABLE I  
PROCESS DATA AND RESULTS FOR SPD ON THE SPECIAL COMB-DRIVE  
RESONATORS AT 3.5 V INPUT

Sample	$f_0$ (kHz)	$R_0$	Process Time (mins)	Power Dissipation (mW)		Length of Hotspot
				$P_{avg}$	$P_{max}-P_{min}$	
1	84.7	845	15	10.5	0.4	38
2	87.5	843	10	10.1	0.5	40
3	86.2	770	4	10.4	0.5	44
4	86.6	779	2	10.3	0.5	46
5	87.2	793	5	10.7	1.6	56
6	87.9	785	5	10.4	0.8	65
7	86.5	790	15	10.7	1.2	73

were fabricated using the Cronos MUMPs in the Poly 1 layer, which was  $2 \mu\text{m}$  thick and suspended  $2 \mu\text{m}$  from the substrate. The resonators were released in HF, followed by supercritical  $\text{CO}_2$  drying. Frequency measurements (before and after SPD) were made at atmospheric pressure by applying 20 Vpp-ac to the stator and 40 V-dc to the rotor and observing motion under an optical microscope. Seven samples were tested. Their average initial resonant frequency was 86.6 kHz. The uncertainty in frequency measurements was  $\pm 50$  Hz. In the SPD trials, silane was introduced at 100 sccm and 150 mtorr, a lower pressure than the previous procedure to obtain better selectivity and finer grain structure. Power was applied at constant voltage (3.5 V) for various lengths of time, from 2 to 15 min, as listed on Table I. The output current was recorded using an HP semiconductor analyzer and power dissipation was computed.

### B. Results and Discussion

Polysilicon was selectively deposited on the single beam of the rotors as shown in Fig. 5 for Sample 7. In this case, resonant frequency increased  $\approx 1700$  Hz or 1.96%. The quality factor (Q) of the resonator was not measured, but it is expected to increase substantially because localized, post-fabrication heating has been shown to do so [8]. Also, Q is proportional to  $\sqrt{k_s/m}$ , where  $k_s$  is stiffness and  $m$  is mass. Both quantities are increased in the process. It should be noted that the new film has good adhesion to the substrate. It withstood high frequency vibration for repeated measurements without delaminating. A cross section was made through the old and new films [14]. The interface showed no cracking.

Fig. 6 is a comparison of the results for all the samples. When the location of the new deposition was marked on the SEM and

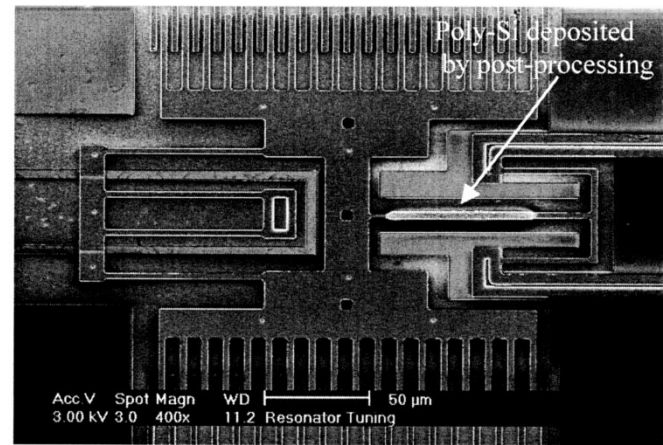


Fig. 5. Selective deposition on Sample 7.

aligned, the samples with the longer hotspots (area containing SPD) showed larger changes in resonant frequency. The percent change in resonant frequency ( $\Delta f_r$ ) ranged from 0.7 to 2.0%. The initial resonant frequencies are given on Table I, along with the length of the hotspots, which varied from  $38 \mu\text{m}$  for Sample 1 to  $73 \mu\text{m}$  for Sample 7. To understand why the length of the hotspot correlates to the  $\Delta f_r$ , consider that resonant frequency is a function of  $k_s/m$ . Mass was increased by the process. Since resonant frequency also increased, the essential effect of the process was an increase in the stiffness of the rotor. Stiffness is a function of size. Increasing the cross section of the single beam in the hotspot increased the stiffness of the rotor. Therefore, longer hotspots yield larger increases in stiffness and resonant frequency.

Consider how adding material to the center of the rotor, as opposed to one of the rotor's suspension beams, would affect resonant frequency. If material were added to the center of the rotor, resonant frequency would decrease because the effect of the added mass would dominate in the  $k_s/m$  ratio. Also, much larger amounts would have to be deposited to obtain the same magnitude of change as shown in the experiments here.

A means of controlling the length of the hotspot was found by examining the power dissipation during the SPD trials. Recall that 3.5 V were applied across each rotor, continuously. The resulting power dissipation profiles are shown in Fig. 7. The power dissipation gives an indicate the relative temperature of the samples. In a heat transfer simulation, using the power outputs, the peak temperatures were found to be 800–900 °C at the center of the hotspots [14]. The thermal responses are not identical because of variation in the initial properties and conditions of the samples, such as the resistance (given in Table I), thermal and electrical conductivities, and the separation of the rotor from the substrate. The sharp fluctuations in the power dissipation may be the result of recrystallization of the heated rotor, the addition of material and changes in the separation of the rotor from the substrate. Despite the variations in thermal response, the average power dissipation results (given in Table I) were quite consistent, ranging from 10.1 to 10.7 mW. It was found that the length of the hotspots correlated to the maximum difference in power dissipation, ( $P_{max} - P_{min}$ ), during each trial, as shown on Table I. Other factors such as the initial, final or average power

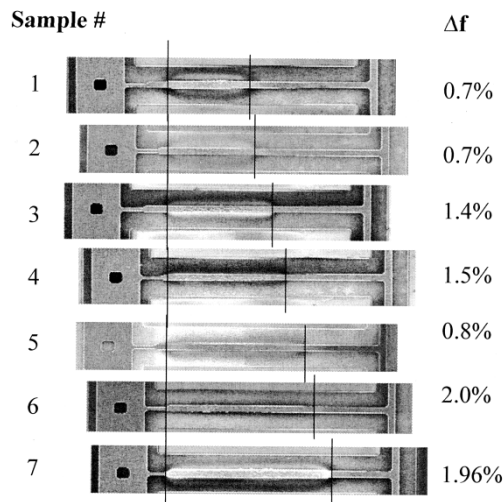


Fig. 6. The correlation between the size of the hotspots and the change in frequency. All SEMs are magnified 400X.

dissipation and time do not show as strong a correlation with the length of the hotspot. Since the length of the hotspots also correlates to the  $\Delta f_r$ , controlling the magnitude of change in the power dissipation appears to be an avenue to tuning resonant frequency. This will be discussed further in the section on tuning to a target frequency.

One sample produced discrepancies in the trends described above. An explanation indicates the other factors affecting resonant frequency. For Sample 5, the  $\Delta f_r$  (0.8%) was much less than expected from comparison of the length of the hotspots in Fig. 6. Sample 5 also had the largest fluctuation in power dissipation during its SPD trial. The second largest fluctuation in power dissipation was found in Sample 7, and the smallest in Sample 1. In comparing close-up SEM of Samples 1, 5, and 7 (shown in Fig. 8(b), (c), and (d), respectively), a slight upward deflection was apparent in the single beam of Sample 5. It seems the larger fluctuation in power dissipation (and thermal load) caused more strain. No permanent strain is evident in Sample 1 and Sample 7 or the other samples. Therefore, there is evidence that resonant frequency was affected by the increased permanent strain and residual stress in the rotor.<sup>2</sup>

The residual stress in the rotor is caused by nonuniform heating of the single beam. As the rotor is heated, the material in the hotspot wants to expand, but is constrained by the surrounding material. So it experiences compressive stress. When the rotor cools, the hotspot lags the surrounding material. It cannot fully contract and is left with tensile residual stress.<sup>3</sup>

The material surrounding the hotspot assumes compressive residual stress so that forces on the rotor balance [22].

When the added material is also considered during the nonuniform heating of the beam, various arguments [23],

<sup>2</sup>This argument is made assuming that the added volume of polysilicon, but not its texture, determines the  $\Delta F_r$  and assuming the density of polysilicon is invariant.

<sup>3</sup>A similar conclusion was reached by Chen et al. [20] by examining the curved load path of heated materials in stress-strain space and their reduction in Young's Modulus. The Young's Modulus of the MUMP's polysilicon decreases 10% over the temperature range 0–250 °C [21]. One can assume that at 800 °C, it is 30% less than the room temperature value, giving an indication of the extent to which the elastic behavior is nonlinear.

[24] can be made about the sign of the residual stress in the hotspot. It depends on the temperature coefficient of expansion of the new film, the reduction in stress from the increasing cross-section, the reaction forces at the anchors of the rotor and the rotor's initial residual stress. The experiments here indicate the  $\Delta f_r$  will follow the correlation with the length of the hotspot until the residual stress reaches a certain level. At this level, strain is observable, as in Sample 5. Samples 1–4, 6 and 7 are considered to be below that level. In the next section, an attempt was made to determine the effect of localized heating alone on the resonant frequency.

#### IV. MODIFYING FREQUENCY BY LOCALIZED ANNEALING

Localized annealing seems to change resonant frequency by altering residual stress. The following experiment was performed for comparison to the results of the SPD process.

##### A. Procedure

A special comb-drive resonator, Sample 8, was placed in a CVD chamber and nitrogen was introduced to a pressure of 150 mtorr. As with the selective deposition trials, power was applied at constant voltage (3.5 V). The process time was 5 min. The output current was recorded using an HP semiconductor analyzer and power dissipation was computed.

##### B. Results and Discussion

After the localized annealing process, the resonant frequency of Sample 8 (initially 88.3 kHz) increased 1%, but the surface of the single beam also changed, as shown in Fig. 9. Voids appeared in the hotspot, along grain boundaries, and the area was blanched. The average power dissipation during the trial was 10.0 mW, slightly less than those of the selective deposition trials. The polysilicon beam's response in the inert gas environment is not yet understood. The localized annealing trial was repeated (power was applied gradually from 0 to 10 mW) on a special comb-drive resonator (Sample 9) in an argon-filled chamber at 150 mtorr. The resonant frequency (initially 86.6 kHz) increased in 0.8%, and voids were also found in the hotspot on the single beam [14]. Since mass was reduced in these trials, the desired data on the  $\Delta f_r$  due to heating alone were confounded.

In the investigation of localized annealing by Wang *et al.* [8], there was no mention of a change in the volume or the surface of the polysilicon rotor, and the power dissipation was not reported, but an increase in resonant frequency was also reported.

In this work, the localized annealing process and SPD at high temperatures have been shown to create distortions in the resonator. Therefore, the recommended procedure for modifying resonant frequency permanently is the selective polysilicon deposition process at low temperatures to minimize the effect on residual stress. The steady and predictable effect of adding material to the rotor is shown using the simulation in the next section.

#### V. EFFECT OF ADDING MATERIAL

A finite element simulation was developed to determine the  $\Delta f_r$  due to the added material alone. ABAQUS beam and shell

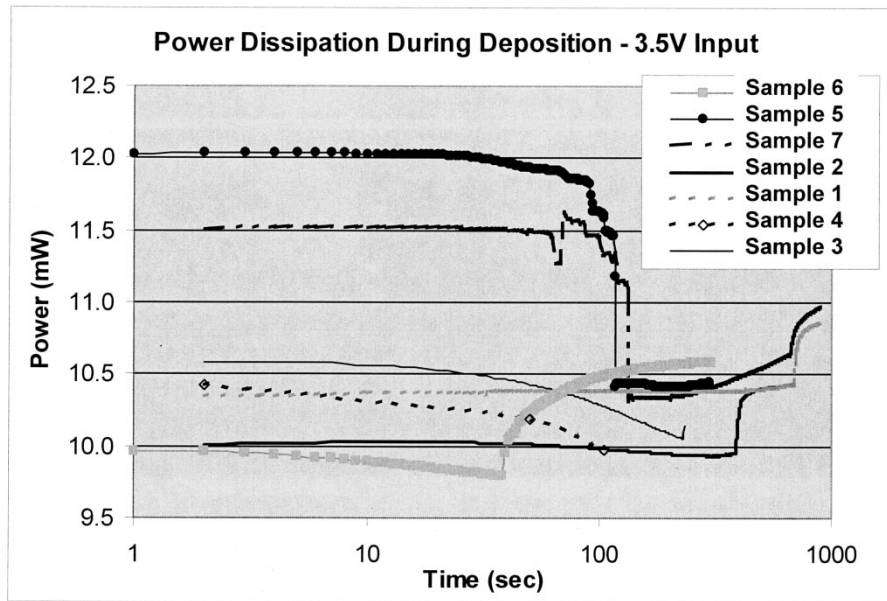


Fig. 7. Power dissipation during SPD on special comb-drive resonators.

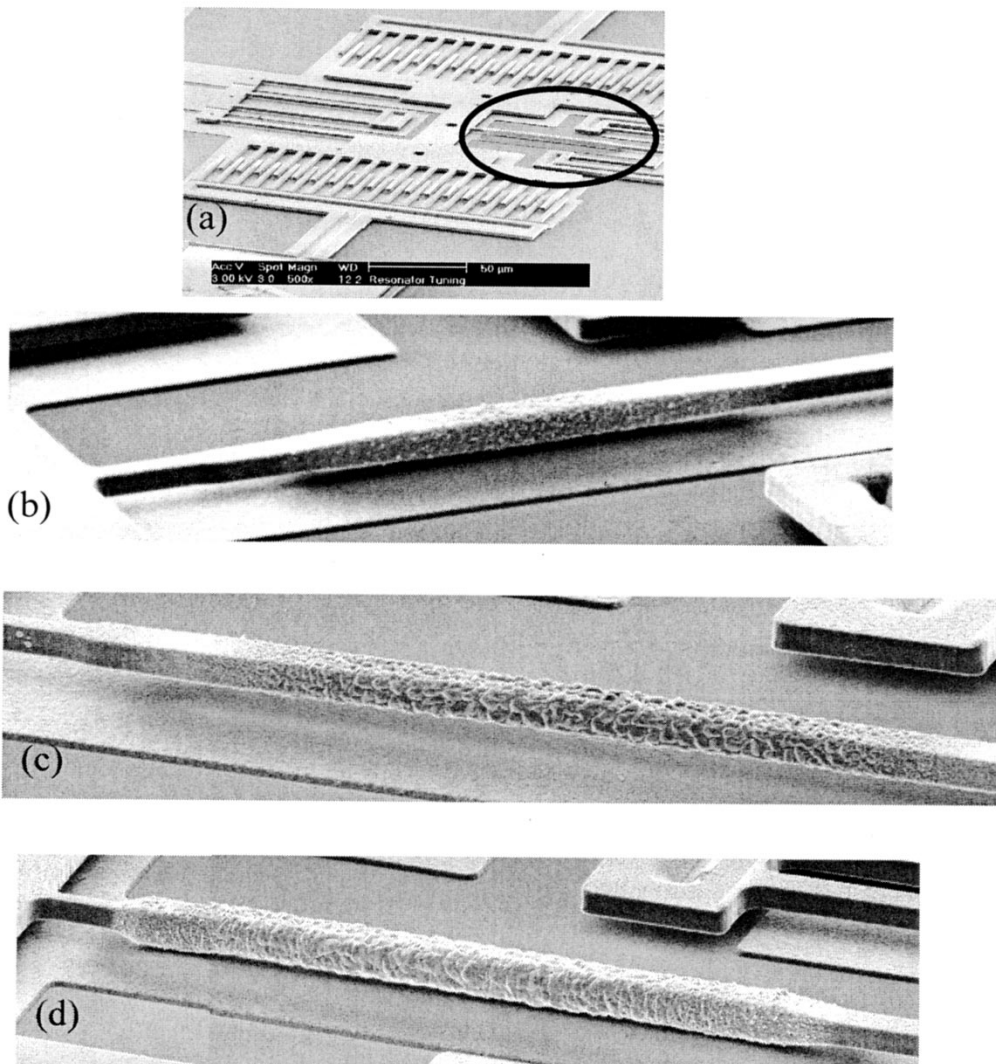


Fig. 8. Close-up views of SPD on (a) Sample 7, (b) Sample 1 at 1600X, (c) Sample 5 at 2000X, and (d) Sample 7 at 2000X.

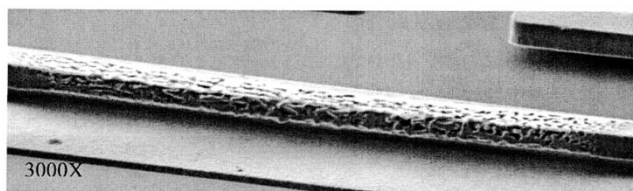


Fig. 9. Result of localized annealing on the single beam of Sample 8.

elements [25] were used to model the special comb-drive resonator. The hotspot was defined by the ‘extent of spot’ and the ‘spot separation’, as shown in Fig. 10. The size of the hotspot was modified in the simulation, assuming the thickness of the added material was uniformly  $0.3 \mu\text{m}$ , which is an approximation of the results of Sample 7.

The simulation confirmed the experimental finding that the longer the hotspot, the larger the  $\Delta f_r$ . The simulation also showed the  $\Delta f_r$  increases as the spot separation decreases. In fact, as the hotspot approaches either end of the single beam, the  $\Delta f_r$  increases. Flexural rigidity is being increased where the bending moment is greatest. Adding material to the center of the single beam is not as effective. A segment of the single beam, between spot separations 0 and  $10 \mu\text{m}$  (away from the heat sinks at the anchors), was reduced in size to increase temperature and promote deposition in this location. In Fig. 10, the curves have steeper slopes when material is added in this reduced segment.

The simulation was used to check the results for Sample 7. At the star in Fig. 10, the spot separation is  $8 \mu\text{m}$  and the extent of spot is  $80 \mu\text{m}$ . The calculated change in frequency was 2.2%, which is in good agreement with the measured value of 1.96%. Thus, designing the resonator to target a particular location for the added material should be a priority. For example, without the reduced section, heat transfer simulations indicate the spot separation for Sample 7 would increase to  $18 \mu\text{m}$ . The  $\Delta f_r$  would be 0.5%. Fig. 10 shows that if the hotspot in Sample 7 began at the spot separation of 0, the  $\Delta f_r$  would increase to 9%. Polysilicon is one of the few materials with which a  $\Delta f_r$  this high could be achieved by the addition of only  $0.3 \mu\text{m}$  to the surfaces of the single beam. Its advantage is its high specific modulus- ten times higher than that of platinum, another material that has been selectively deposited. Selectively depositing polysilicon is a good choice for getting the greatest  $\Delta f_r$  with the least amount of added material.

## VI. TUNING TO A TARGET FREQUENCY

Additional experiments may yield explicit relations of the correlations above, but the potential for tuning resonant frequency to a particular value is already apparent. The following is a guideline for continuing research. Consider tuning Samples 1 and 2, from their original resonant frequencies to say, 88.0 kHz. The required  $\Delta f_r$ 's are 3.9% and 0.6%, respectively. Plan to make the selectively deposited film  $0.3 \mu\text{m}$  thick and use Fig. 10 to determine the dimensions of the hotspots. A horizontal line, on Fig. 10, at the required  $\Delta f_r$  intersects several possible combinations of spot separation and extent of spot. Choose the smallest spot separation because it can be achieved

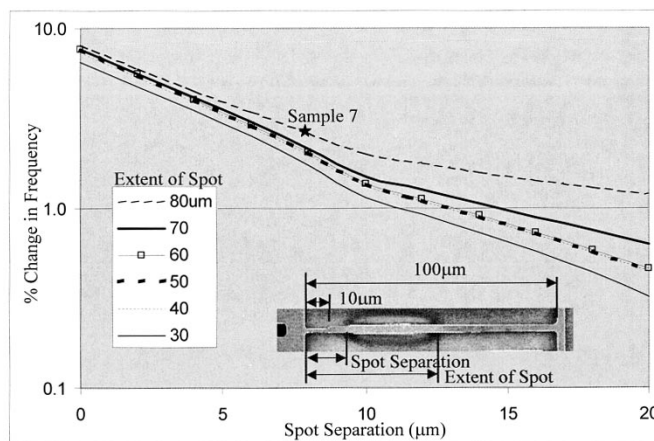


Fig. 10. Simulation of the change in resonant frequency for changes in the location of deposition. The thickness of the new film is  $0.3 \mu\text{m}$ .

at the lowest temperature. These results define the length of the hotspots.

To produce these hotspots, do SPD trials while controlling the power dissipation. The data on Table I show a correlation between the maximum change in power dissipation,  $\Delta p$ , and the length of the hotspot. Interpolate to determine  $\Delta p$  for each hotspot. Apply 3.5 V to the samples in a gradual ramp-up. Use a control circuit to limit the maximum power dissipation to 10 mW and minimum to  $(10\text{mW} - \Delta p)$ . Using the anticipated average power dissipation and a thermal simulation, predict temperature and use that to estimate deposition rate. Allow the process to continue for a time determined by the desired film thickness and the deposition rate of the silane/helium mixture. Attempt deposition in one shot; the effects of numerous thermal cycles enormously complicate predictions. These recommendations are a probable path to matching the resonant frequencies of the MEMS. Several experimental trials, supported by simulations, are required for precise tuning.

## VII. CONCLUSION

A postfabrication process has been proposed for the frequency tuning of microresonators. The selective deposition of polysilicon was demonstrated on two designs. It was found that:

- the change in resonant frequency depends on the length of the hotspots and the residual stress induced in the rotor;
- the effects of the added material alone and heating alone were examined;
- the length of the hotspots correlated to the magnitude of the power fluctuation;
- residual stress was negligible for trials with low power dissipation;
- these data provide a path to controlling resonant frequency by adding material.

## ACKNOWLEDGMENT

The authors wish to thank Prof. R. A. Scott of the University of Michigan for advice on conducting the research and the finite

element simulations, and Prof. K. D. Wise of the University of Michigan for use of equipment in his lab.

#### REFERENCES

- [1] E. C. Harvey, "Laser micromachining," in *Proc. 1997 IEEE Colloquium on Microengineering Technologies and How To Exploit Them*, 1997.
- [2] S. Majoo, J. W. Schwank, J. L. Gland, and K. D. Wise, "Selected-area CVD method for deposition of sensing films on monolithically integrated gas detectors," *IEEE Electron Device Lett.*, vol. 16, pp. 217–219, 1995.
- [3] R. Manginell, J. H. Smith, A. J. Ricco, D. J. Moreno, R. C. Hughes, R. J. Huber, and S. D. Senturia, "Selective, pulsed CVD of platinum on microfilament gas sensors," in *Proc. 1996 Solid-State Sensor and Actuator Workshop (Hilton Head, S.C.)*, 1996, pp. 23–27.
- [4] R. E. Cavicchi, J. S. Suehle, P. Chaparala, K. G. Kreider, M. Gaitan, and S. Semancik, "Microhotplate gas sensor," in *Proc. 1994 Solid State Sensor and Actuator Workshop (Hilton Head, S.C.)*, 1994, pp. 53–56.
- [5] C. W. Seabury, J. T. Cheung, P. H. Kobrin, R. Addison, and D. P. Havens, "High performance microwave air-bridge resonators," in *Proc. IEEE Ultrasonics Symposium*, vol. 2, 1995, pp. 909–911.
- [6] S. Wolf and R. N. Tauber, *Silicon Processing for the VLSI Era, Volume 1: Process Technology*: Lattice Press, 1986, p. 401.
- [7] J. J. Yao and N. MacDonald, "A micromachined, single-crystal silicon tunable resonator," *J. Microelectromech. Syst.*, vol. 6, Dec. 1996.
- [8] K. Wang, A.-C. Wong, W.-T. Hsu, and C.T.-C. Nguyen, "Frequency trimming and Q-factor enhancement of micromechanical resonators via localized filament annealing," in *Proc. 1997 Int. Conference on Solid-State Sensors and Actuators Transducers '97*, pp. 109–112.
- [9] K. Tanaka, Y. Mochida, M. Sugimoto, K. Moriya, T. Hasegawa, K. Atsuchi, and K. Ohwada, "A micromachined vibrating gyroscope," *Sens. Actuators, Phys. A*, vol. 50, pp. 111–115, 1995.
- [10] D. Joachim and L. Lin, "Localized CVD of poly-crystalline silicon for post-fabrication processing," in *Proc. MEMS Symposium, 1999 ASME International Mechanical Engineering Congress and Exposition*, vol. 1, Nov. 1999, pp. 37–42.
- [11] —, "Design of MEMS resonators for tuning with selective polysilicon deposition," in *Proc. MEMS Symposium, 2001 ASME International Mechanical Engineering Congress and Exposition*, vol. 2, Nov. 2001, CD ROM.
- [12] D. Joachim and L. Lin, "Selective polysilicon deposition for frequency tuning of MEMS resonators," in *Proc. IEEE Micro Electro Mechanical Systems Conference, 2002*, pp. 727–730.
- [13] L'air Liquide: Division Scientifique, *Encyclopedie Des Gaz*: Elsevier, English Translation.
- [14] D. Joachim, "Selective deposition of polycrystalline silicon for tuning micro-electro-mechanical resonators: Experiment and simulation," Ph.D. dissertation, Univ. Michigan, Ann Arbor, 2001.
- [15] *Multi User MEMS Processes (MUMP's) Design Handbook*, 2001.
- [16] C. H. Mastrangelo, "Thermal applications of Microbridges," Ph.D. dissertation, Univ. California, Berkeley, 1991.
- [17] R. C. Jaeger, "Introduction to microelectronic fabrication," in *Modular Series on Solid State Devices*. Reading, MA: Addison-Wesley, 1993, vol. 5, p. 122.
- [18] T. M. Bloomstein and D. J. Ehrlich, "Laser deposition and etching of three-dimensional microstructures," in *Proc. 1991 Int. Conference on Solid-State Sensors and Actuators, Transducers '91*, pp. 507–511.
- [19] T. I. Klamins, *Polycrystalline Silicon for Integrated Circuits and Displays*. New York: Kluwer Academic, 1998, p. 151.
- [20] G. Chen, X. Xu, C. C. Poon, and A. C. Tam, "Laser assisted high precision curvature modification of ceramics and steels," *Opt. Eng.*, vol. 37, pp. 2837–2842, 1998.
- [21] W. N. Sharpe jr., M. A. Eby, and G. Coles, "Effect of temperature on mechanical properties of polysilicon," in *Proc. 2001 Int. Conference on Solid-State Sensors and Actuators, Transducers '01*, pp. 1366–1329.
- [22] E. P. DeGarmo, J. T. Black, and R. A. Kohser, *Materials and Processes in Manufacturing*. New York: MacMillan, 1988, p. 959.
- [23] H. Guckel, D. W. Burns, C. C. G. Visser, H. A. C. Tilmans, and D. DeRoo, "Fine grained polysilicon with built-in tensile strain," *IEEE Trans. Electron Dev.*, vol. 35, no. 6, pp. 18–19, June 1988.
- [24] Y.-H. Min and Y.-K. Kim, "A synchronous technique for determination of residual stresses in micromachined thin films using composite layer," in *Proc. 1999 Int. Conference on Solid-State Sensors and Actuators, Transducers '99*, pp. 458–461.
- [25] *ABAQUS/Standard, Version 5.8*, 1998.



**Daphne Joachim** received the B.Eng. degree in mechanical engineering from The Cooper Union, New York City, NY, in 1991 and the M.S. degree in mechanical engineering at Stanford University, Stanford, CA, in 1993. She received the Ph.D. degree in mechanical engineering from the University of Michigan, Ann Arbor, in 2001 with research focused on electrostatic microresonators, multidomain finite element analysis, and heat transfer in polysilicon.

She worked as a manufacturing engineer for General Motors and is a registered engineer in the State of Michigan. She currently works on microsystems modeling at Sandia National Laboratories, Livermore, CA.

Dr. Joachim is a Member of the American Society of Mechanical Engineers (ASME).



**Liwei Lin** (S'92–M'93) received the M.S. and Ph.D. degrees in mechanical engineering from the University of California, Berkeley, in 1991 and 1993, respectively.

From 1993 to 1994, he was with BEI Electronics, Inc., USA, in research and development of microsensors. From 1994 to 1996, he was an Associate Professor in the Institute of Applied Mechanics, National Taiwan University, Taiwan. From 1996 to 1999, he was an Assistant Professor at the Mechanical Engineering and Applied Mechanics Department at the University of Michigan, Ann Arbor. In 1999, he joined the University of California at Berkeley and is now an Associate Professor at Mechanical Engineering Department and Co-Director at Berkeley Sensor and Actuator Center, NSF/Industry/University research cooperative center. His research interests are in design, modeling, and fabrication of microstructures, microsensors, and microactuators as well as mechanical issues in microelectromechanical systems including heat transfer, solid/fluid mechanics, and dynamics. He holds eight U.S. patents in the area of MEMS.

Dr. Lin is the recipient of the 1998 NSF CAREER Award for research in MEMS Packaging and the 1999 ASME *Journal of Heat Transfer* Best Paper Award for his work on microscale bubble formation. He served as Chairman of the Micromechanical Systems Panel of the ASME Dynamic Systems and Control Division in 1997 and 1998 and led the effort in establishing the MEMS subdivision in ASME and is currently the Vice Chairman of the Executive Committee.